China Instrument and Control Society
Instrumentation
INSTRUMENTATION, Vol. 12, No. 2, June 2025
https://doi.org/10.15878/j.instr.202500243

Article

High-Precision Localization Method for Spheres with a Theodolite

Junfeng Sun[1], Qihua Huang[1], Lianyou An[1], Jinling Kang[1], Baolu Wang[2,*], Huanlong Zhang[2]

[1] China Tobacco Guangxi Industrial Co., LTD.Nanning, Guangxi 530000, China

[2] Zhengzhou University of Light Industry Dongfeng Road, Zhengzhou, Henan 450002, China

[*] Corresponding author email: 332301020031@zzuli.edu.cn

Abstract: Spherical objects are widely used in target localization applications, and the existing sphere localization methods with cameras or total stations both have some limitations. A new high-precision sphere localization method with a theodolite is proposed in this paper. From the view point of the theodolite, the contour points of a sphere with a known radius are measured as latitude-longitude coordinates. It is observed that the center of the target sphere is located on a cylindrical surface constructed with the latitude-longitude coordinates, and therefore the latitude-longitude coordinates of at least three contour points can be used to construct a set of ternary quadratic equations. The Gröbner basis method is used to compute at most four real solutions of the sphere center coordinates. To distinguish the only meaningful solution from the other possible real solutions, a pre-processing of the measured longitude values is also proposed. The factors affecting the positioning accuracy of the sphere center are evaluated in simulation experiments, which are used to obtain an empirical estimation model of the positioning error. Real data experiments are also performed and the results show that the proposed method can achieve high localization precision.

Keywords: sphere localization; latitude-longitude coordinates; gröbner basis; empirical estimation model

Citation: Junfeng Sun, Qihua Huang, Lianyou An, Jinling Kang, Baolu Wang, Huanlong Zhang."High-Precision Localization Method for Spheres with a Theodolite." Instrumentation 12, no.2 (June 2025). https://doi.org/10.15878/j.instr.202500243

1 Introduction

A sphere is an object with rotational symmetry. This property of the sphere makes its image display a good contour continuity, so that it can adapt to any angle of shooting. Based on this feature of spheres, the positioning technique of spherical targets has received extensive attention and research in recent years. This fact promotes the development of the technology and makes it applicable in camera calibration and object localization [1-5].

At present, researchers have already proposed methods of sphere localization based on the image of the target sphere with a known radius. Most of the methods require obtaining the coordinates of the projection point of the sphere center by using the edge points of the image[2,6], or the ellipse center and area of the image[7,8]. Then, the target sphere center can be extracted by constructing a positive cone tangent to the sphere[9,10]. In addition, a method of directly solving the center of the sphere based on the Gröbner basis method has also been proposed[11]. The above methods require high-precision camera calibration and lens distortion correction[12-15], and a longer focal length of the camera can increase the positioning accuracy of the target sphere while decreasing the maximal field of view angle.

The total station method has also been widely used in engineering practice. For example, Kim et al.[16] used the total station automatic tracking technology based on the principle of tracking 360-degree prism targets to locate drones in complex environments. Osada et al.[17] derived the Gauss-Helmert observation model and achieved the direct positioning of the total station in the geocentric coordinates system. In addition, Chen et al.[18] applied the total station measurement to locate the center of the welded sphere. This method requires the use of a total station to obtain the three-dimensional coordinates of a

reference point with the aid of a gradient, and then acquire the sphere center coordinates from the geometric relationship between the center of the sphere and the reference point. Although this method has a smaller positioning error of the sphere center than visual positioning methods using a sphere image, the production of the auxiliary device increases the positioning cost. Moreover, the laser ranging accuracy of the total station is limited by its electronic components, which are usually in millimeters.

Compared with the total station, the theodolite has similar angle measurement accuracy and is relatively low in price, so it is also favored in engineering practice. Fu et al. [19] achieved single theodolite positioning of close-range targets by identifying three known feature points on the target. Gong et al. [20] proposed an improved multi-station theodolite positioning method based on Hermite function constraints. Fang et al.[21] used four rotating laser theodolites to construct a combined laser three-dimensional scanning system, which is suitable for on-site measurement without guide rails. Zhao[22] proposed a multi-station optoelectronic theodolite rendezvous positioning method based on the fusion of dynamic weighting given the deficiency of the traditional idealized rendezvous positioning model.

In this article, a high-precision positioning method for spherical targets is proposed taking advantage of the high-precision angle measurement feature of the theodolite. This method uses the sphere radius and the latitude-longitude coordinates of its contour point to construct a cylindrical surface model containing the center of the sphere. From this model, the sphere center coordinates can be solved as the intersection of three cylindrical surfaces. Since the latitude-longitude coordinates of the sphere contour points can be measured with low error, the proposed method can effectively reduce the system positioning error. Compared with the existing image method and total station method, the proposed method has the benefits of easy operation, high positioning accuracy, and low cost.

2 Positioning Model and Three-point Method for the Sphere Center

2.1 A Cylindrical Model Containing the Sphere Center

A sphere has a good rotational symmetry in space, so its contour in the theodolite is a standard circle, marked $\boldsymbol{C}$. For the i^{th} contour point $\boldsymbol{P}_i$ on the circle with i= 1, 2, 3, $\cdots N$, the latitude-longitude coordinates are measured as $(H_i,V_i)^{\mathrm{T}}$. Here, H_i is a horizontal angle in the range from 0 to 2π and V_i is a vertical angle in the range from -0.5π to 0.5π.

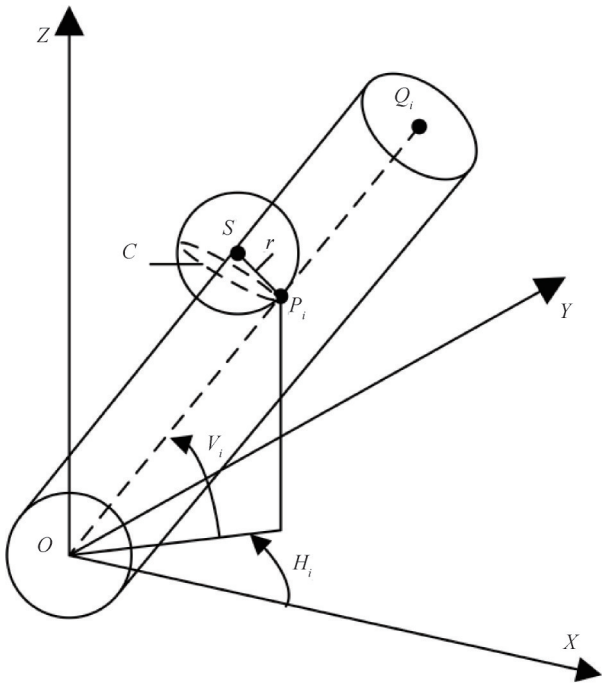

Fig.1 A cylindrical model containing the center of the target sphere.

As shown in Fig. 1, in the Cartesian coordinate system with the center of the theodolite $\boldsymbol{O}$ as the origin, a unit direction vector $\boldsymbol{Q_i}$ is obtained according to the latitude-longitude coordinates of the i^{th} contour point $\boldsymbol{P_i}$. The elements of $\boldsymbol{Q_i}=(l_i,m_i,n_i)^{\mathrm{T}}$ can be calculated as

$$\begin{cases} l_i=\cos(V_i)\cos(H_i) \\ m_i=\cos(V_i)\sin(H_i). \\ n_i=\sin(V_i) \end{cases} \tag{1}$$

Let r be the sphere radius, and then the sphere center $\boldsymbol{S}=(X,Y,Z)^{\mathrm{T}}$ satisfies the following constraint:

$$\left|S\times Q_i\right|^2=r^2\left|Q_i\right|^2, \tag{2}$$

which can be rewritten as

$$\begin{aligned}&\left(m_i^2+n_i^2\right)X^2-2l_im_iXY-2l_in_iXZ+\left(l_i^2+n_i^2\right)Y^2\\&-2m_in_iYZ+\left(l_i^2+m_i^2\right)Z^2=r^2\left(l_i^2+m_i^2+n_i^2\right)\end{aligned} \tag{3}$$

Equation (3) shows that a ternary quadratic equation concerning the sphere center coordinates can be obtained from each contour point.

2.2 Three-Point Method for Sphere Center Positioning

When the number of measured contour points $N\geqslant 3$, by stacking a set of equations in the form of (3), we have

$$\begin{bmatrix} m_1^2+n_1^2,-2l_1m_1,-2l_1n_1,l_1^2+n_1^2,-2m_1n_1,l_1^2+m_1^2 \\ m_2^2+n_2^2,-2l_2m_2,-2l_2n_2,l_2^2+n_2^2,-2m_2n_2,l_2^2+m_2^2 \\ \vdots \\ m_N^2+n_N^2,-2l_Nm_N,-2l_Nn_N,l_N^2+n_N^2,-2m_Nn_N,l_N^2+m_N^2 \end{bmatrix}\begin{bmatrix} X^2 \\ XY \\ XZ \\ Y^2 \\ YZ \\ Z^2 \end{bmatrix}=\begin{bmatrix} r^2\left(l_1^2+m_1^2+n_1^2\right) \\ r^2\left(l_2^2+m_2^2+n_2^2\right) \\ \vdots \\ r^2\left(l_N^2+m_N^2+n_N^2\right) \end{bmatrix} \tag{4}$$

The system of equations is similar to the set of equations constructed in[11]. It can be written as $\boldsymbol{AW}=\boldsymbol{b}$, where $\boldsymbol{A}$ is an $N\times 6$ matrix, $\boldsymbol{b}$ is an $N\times 1$ vector, and $\boldsymbol{W}$ is the 6-vector $[X^2, XY, XZ, Y^2, YZ, Z^2]^{\mathrm{T}}$. Let $\boldsymbol{V}_1$, $\boldsymbol{V}_2$, and $\boldsymbol{V}_3$ be the three singular vectors of $\boldsymbol{A}$ corresponding to the three smallest singular values no matter $N=3$ or $N>3$. The solution of the system of equations can be expressed as

$$W = k_1 V_1 + k_2 V_2 + k_3 V_3 + W_0. \tag{5}$$

Here, $\boldsymbol{W}_0=\boldsymbol{A}^{+}\boldsymbol{b}$ is a particular solution, where $\boldsymbol{A}^{+}$ is the pseudo-inverse of $\boldsymbol{A}$. The process of solving the (4) can be transformed to solving the three unknowns (k_1, k_2, k_3) in (5). Let $\boldsymbol{W}=[\omega_1, \omega_2, \omega_3, \omega_4, \omega_5, \omega_6]^{\mathrm{T}}$ and construct a set of equations according to the relationship between the six entries of vector $\boldsymbol{W}$, as shown below:

$$\begin{cases} \omega_1\omega_4 - \omega_2^2 = 0 \\ \omega_1\omega_6 - \omega_3^2 = 0 \\ \omega_4\omega_6 - \omega_5^2 = 0 \\ \omega_2\omega_3 - \omega_1\omega_5 = 0 \\ \omega_2\omega_5 - \omega_4\omega_3 = 0 \\ \omega_3\omega_5 - \omega_6\omega_2 = 0 \end{cases}. \tag{6}$$

Equations (6) are six ternary quadratic equations with the unknowns (k_1, k_2, k_3), and the Gröbner basis method[11, 25] is used to obtain all the real solutions. Define the monomials vector

$$K_s = \left[k_1^2, k_1k_2, k_1k_3, k_2^2, k_2k_3, k_3^2, k_1, k_2, k_3, 1\right]. \tag{7}$$

It is now possible to rewrite (6) as

$$MK_s = 0 \tag{8}$$

where $\boldsymbol{M}$ is a 6×10 matrix. After Gauss-Jordan's elimination, (8) can be rewritten as

$$\left[I \quad B\right]K_S = 0. \tag{9}$$

Here, $\boldsymbol{I}$ is the 6×6 identity matrix and $\boldsymbol{B}$ is a 6×4 matrix. Define the basis monomials vector as

$$u = \left[k_1, k_2, k_3, 1\right]^T. \tag{10}$$

Construct the action matrix $\boldsymbol{A}_k$ from (9) so that

$$ku = A_k u, k \in \{k_1, k_2, k_3\}. \tag{11}$$

Here, the elements in $\boldsymbol{A}_k$ can be expressed with the elements in $\boldsymbol{B}$ according to the choice of k. Denote the j^{th} row of $\boldsymbol{B}$ as $\boldsymbol{b}_j$, and then when k_1, k_2, and k_3 is used respectively, the three versions of $\boldsymbol{A}_k$ are computed as

$$\begin{pmatrix} -b_1 \\ -b_2 \\ -b_3 \\ [1,0,0,0] \end{pmatrix}, \begin{pmatrix} -b_2 \\ -b_4 \\ -b_5 \\ [0,1,0,0] \end{pmatrix}, \begin{pmatrix} -b_3 \\ -b_5 \\ -b_6 \\ [0,0,1,0] \end{pmatrix}. \tag{12}$$

To improve the numerical stability, all the above three matrices are computed, and then the matrix $\boldsymbol{A}_k$ with the largest norm is used to compute $\boldsymbol{u}$. Then, four complex solutions of $\boldsymbol{u}$ can be obtained as the eigenvectors of $\boldsymbol{A}_k$, and the values of the unknown parameters (k_1, k_2, k_3) can be extracted from $\boldsymbol{u}$. Note that the last element of the eigenvectors of the $\boldsymbol{A}_k$ matrix should be normalized to 1.

Next, substitute the real solutions of the three unknowns (k_1, k_2, k_3) into (5). At most four real solutions of $\boldsymbol{W}$ can be obtained, and two sphere center coordinates with opposite signs can be extracted for each real solution of $\boldsymbol{W}$. To distinguish the correct coordinates, it is assumed that the longitude value of the target sphere center is around zero. Now, at most four sphere center coordinates will be obtained from at most four solutions of $\boldsymbol{W}$ as follows:

$$\begin{cases} X = \sqrt{\omega_1} \\ Y = \omega_2 / X \cdot \\ Z = \omega_3 / X \end{cases} \tag{13}$$

Finally, when considering the constraint $X > r$, the target sphere center calculated by the above method usually has one solution.

However, it cannot be guaranteed that the target sphere position always satisfies the above assumption in actuality. A pre-processing for the contour points is necessary to be performed. Here, the horizontal angle after preprocessing is $H_i'=H_i-\overline{H}$, where $\overline{H}$ is the average of the horizontal angles computed as $\overline{H}=1/N(H_1+H_2+\cdots+H_N)$.

Then, at least three measurement points of the form $(H_i', V_i)^{\mathrm{T}}$ are substituted into the aforementioned positioning method, and the sphere center coordinates $(X', Y', Z')^{\mathrm{T}}$ can be obtained in the new coordinate system. Finally, post-processing is performed so that the coordinates $(X, Y, Z)^{\mathrm{T}}$ in the initial Cartesian coordinates system are obtained by the following transform:

$$\begin{bmatrix} X \\ Y \\ Z \end{bmatrix} = \begin{bmatrix} \cos(\tilde{H}) & -\sin(\tilde{H}) & 0 \\ \sin(\tilde{H}) & \cos(\tilde{H}) & 0 \\ 0 & 0 & 1 \end{bmatrix} \begin{bmatrix} X' \\ Y' \\ Z' \end{bmatrix}. \tag{14}$$

2.3 Maximum-Likelihood Estimation

The above solution of the sphere center coordinates is obtained through an analytical method. When more than three contour points are measured, the maximum-likelihood estimate is used as the final refinement scheme.

As shown in Fig. 2, the plane π passing through the straight line $\boldsymbol{OS}$ and perpendicular to the plane XY intersects the circle $\boldsymbol{C}$ at two points. Particularly, one of the two points with the lower vertical angle is denoted as $\boldsymbol{P}_0$. According to the geometric relationship in the right-angled triangle $\boldsymbol{SOP}_0$, we have

$$\begin{cases} |OP_0| = \sqrt{|OS|^2 - r^2} \\ \theta = \arcsin\left(\dfrac{r}{\sqrt{X^2+Y^2+Z^2}}\right) \end{cases}. \tag{15}$$

The latitude-longitude coordinates of the estimated sphere center $\boldsymbol{S}$ can be expressed as

$$\begin{cases} H_S = \arctan 2(Y, X) \\ V_S = \arctan\left(\dfrac{Z}{\sqrt{X^2+Y^2}}\right) \end{cases}, \tag{16}$$

where arctan2 is the arctangent function such that

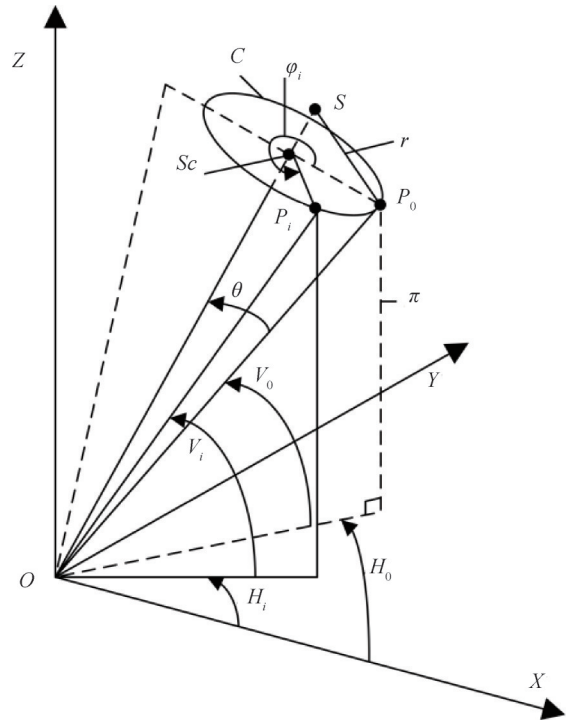

Fig.2 The parameterization of the sphere contour points in the Cartesian coordinate system.

$$\begin{cases} \sin(H_s)=\dfrac{Y}{\sqrt{X^2+Y^2}} \\ \cos(H_s)=\dfrac{X}{\sqrt{X^2+Y^2}} \end{cases}. \tag{17}$$

Now, the Cartesian coordinates of $\boldsymbol{P}_0$ can be expressed as

$$P_0=|OP_0|\begin{bmatrix} \cos(V_s-\theta)\cos(H_s) \\ \cos(V_s-\theta)\sin(H_s) \\ \sin(V_s-\theta) \end{bmatrix}. \tag{18}$$

Since $|\boldsymbol{OP}_0|=|\boldsymbol{OP}_\mathrm{i}|$, the Cartesian coordinates of $\boldsymbol{P}_\mathrm{i}$ can be expressed with the measured latitude-longitude coordinates $(\boldsymbol{H}_i,\boldsymbol{V}_i)$T as

$$P_i=|OP_0|\begin{bmatrix} \cos(V_i)\cos(H_i) \\ \cos(V_i)\sin(H_i) \\ \sin(V_i) \end{bmatrix}. \tag{19}$$

Next, the center of the circle $\boldsymbol{C}$ is computed as

$$S_c=\frac{|OP_0|\cdot|\cos\theta|}{|OS|}S. \tag{20}$$

Denote φ_i as the rotation angle from $\boldsymbol{OP}_0$ to $\boldsymbol{OP}_i$ about the rotation axis $\boldsymbol{OS}_\mathrm{C}$, i.e.

$$\phi_i=\begin{cases} \angle P_0SCP_i, & H_i\geq H_S \\ 2\pi-\angle P_0SCP_i, & H_i<H_S \end{cases}. \tag{21}$$

In the parameterization of the maximum-likelihood, the variables to be refined are $\boldsymbol{S}$ and $\{\varphi_i|i=1,2,3,\cdots,N\}$. Denote $\hat{\boldsymbol{P}}_0$ as the estimated $\boldsymbol{P}_0$ similar to (18), and the estimated value $\hat{\boldsymbol{P}}_i$ of the measurement point can be expressed as

$$\hat{\mathbf{P}}_i=\begin{bmatrix} \hat{x}_i \\ \hat{y}_i \\ \hat{z}_i \end{bmatrix}=R(\hat{\phi}_i os/|os|)\hat{\mathbf{P}}_0, \tag{22}$$

where $\boldsymbol{R}(\hat{\varphi}_i\boldsymbol{OS}/|\boldsymbol{OS}|)$ $\boldsymbol{R}(\hat{\varphi}_i os/|os|)$ is the Rodrigues rotation matrix. Furthermore, the latitude-longitude coordinates can also be obtained by following formula:

$$\begin{cases} \hat{H}_i=\arctan 2(\hat{y}_i,\hat{x}_i) \\ \hat{V}_i=\arctan\left(\dfrac{\hat{z}_i}{\sqrt{\hat{x}_i^2+\hat{y}_i^2}}\right) \end{cases}. \tag{23}$$

The maximum-likelihood estimate can be obtained by minimizing the following cost function:

$$\sum_{i=1}^{N}\left((\hat{H}_i-H_i)^2+(\hat{V}_i-V_i)^2\right), \tag{24}$$

where H_i and V_i are the measurement values, $\hat{\boldsymbol{H}}_i$ and $\hat{V}_i$ are their estimation values as functions of $\boldsymbol{S}$ and $\{\varphi_i|i=1,2,3,\cdots,N\}$. Minimizing (24) is a nonlinear minimization problem of N+3 variables, which is solved with the sparse Levenberg-Marquardt algorithm as described in[29].

In summary, the steps of positioning the target sphere proposed by this paper are as follows:

1) Use a theodolite to measure the latitude-longitude coordinates of at least three approximately uniformly distributed contour points. Then, perform a pre-processing for them such that the average longitude value is zero.

2) Construct a set of ternary quadratic equations with the sphere center coordinates with the cylindrical surface constraint model.

3) Solve the sphere center coordinates using the Gröbner basis method.

4) Extract the correct sphere center coordinates from at most four solutions of the coordinates. Then, the post-processing of the extracted coordinates is performed such that they are represented in the initial Cartesian coordinate system.

5) When the number of measurement points is greater than 3, the optimal solution of the sphere center is calculated by minimizing (24).

3 Validation by Simulation

In this section, we validate the performance of the proposed theodolite method for the positioning of the sphere center by means of simulations, and analyze the factors affecting the sphere center positioning accuracy. In addition, the sphere positioning method with a total station is also performed for comparison.

In the simulation experiments, the initial value of the sphere radius is 10 mm. The latitude-longitude coordinates of the initial position of the target sphere center are $(5, 10)^\mathrm{T}$ in degrees. The initial measurement distance D is 1500 mm. In the initial experimental configuration, the latitude and longitude values of 6

contour points are uniformly sampled, and Gaussian noise with a standard deviation of 2″ is added to the measured angles of the theodolite. Similarly, the angle measurement precision of the total station is also 2″, and its distance measurement precision is 2 mm ± 2 ppm. In each configuration, 1000 repeated tests are performed and then the root mean square error (RMSE) is calculated.

3.1 Number of Contour Points

First of all, we change the number of measurement points in the initial experimental configuration, and investigate the influence of the number of contour measurement points on the sphere positioning accuracy. Here, two methods to sample the measurement points are performed, where the measurement points are uniformly and then randomly selected.

Fig. 3 shows that the proposed method can achieve sphere positioning at least three measurement points. Compared with the traditional total station method, it can obtain higher positioning accuracy under certain experimental conditions. As the number of measurement points increases, the positioning error of the sphere center will also gradually reduce by using the proposed method. By analyzing the data of adjacent measurement samples, it can be found that the positioning error is approximately proportional to the negative 1/2 power of the number of measurement points. Comparing Fig. 3 and Fig. 4, it is not difficult to see that the uniform selection of measurement points has higher positioning accuracy than the random selection, and this difference is particularly obvious when the number of measurement points is small.

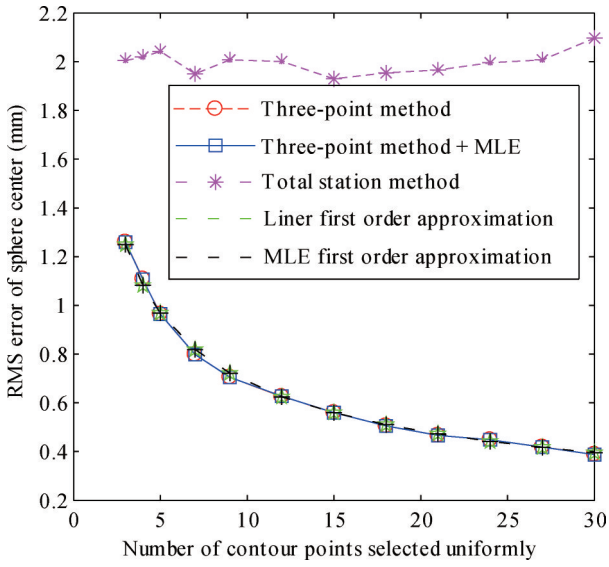

Fig.3 Relationship between the number of the contour points selected uniformly and sphere center error.

3.2 Radius of Sphere

Next, the spheres with different radii are simulated based on the initial configuration to explore the effect of target sphere size on positioning accuracy. Fig. 5 shows

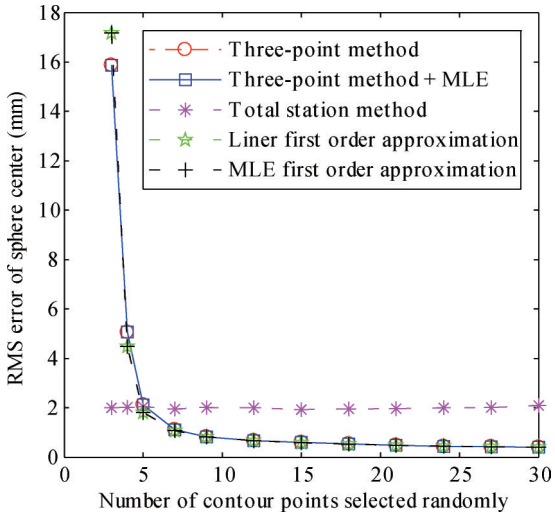

Fig.4 Relationship between the number of the contour points selected randomly and sphere center error.

that, compared with the total station method, the proposed method can obtain higher positioning accuracy under certain experimental conditions. With the gradual increase of the radius, the positioning error of the target sphere continues to decrease. It can be observed that the positioning error of the sphere center is approximately proportional to the inverse of the target sphere radius.

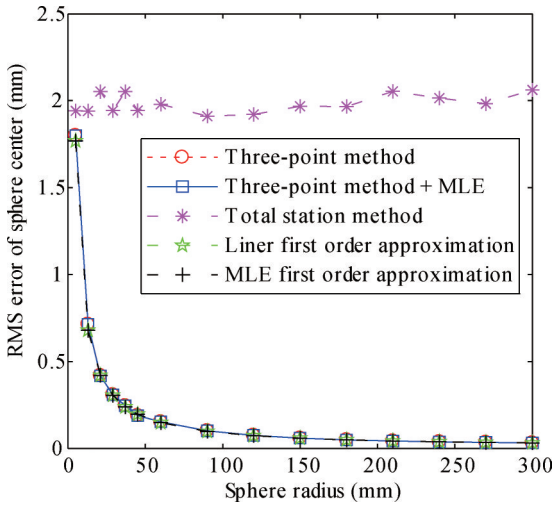

Fig.5 Relationship between sphere radius and sphere center error.

3.3 Distance of Sphere Center

After that, we assume that the measuring distance is sequentially increased from 1000 mm to 3000 mm in the initial configuration and investigate the relationship between measuring distance and positioning error. As can be seen from Fig. 6, when the measuring distance is small, the proposed method has better positioning result than the total station method. It can also be observed that the positioning error is approximately proportional to the square of the measuring distance.

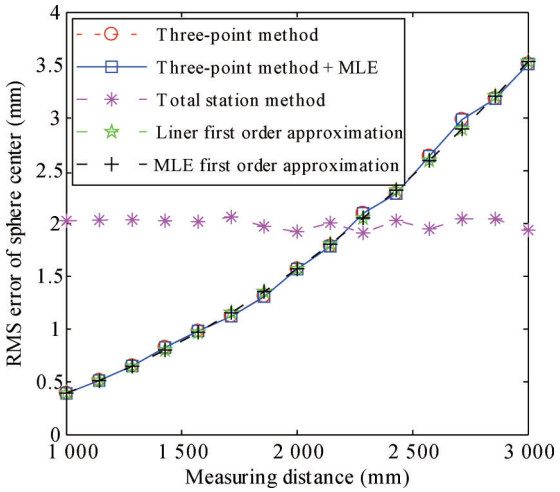

Fig.6 Relationship between measuring distance and sphere center error.

3.4 Vertical Angle of the Sphere Center

Finally, we keep the other initial settings unchanged, and increase the vertical angle of the center of the sphere from −60 degrees to 60 degrees, and calculate the positioning error of the same sphere at different vertical angles one by one. It can be seen from Fig. 7 that the proposed method has higher positioning accuracy than the total station method under certain experimental conditions. The positioning error of the sphere is symmetrical with the vertical angle of the sphere center. When the sphere center is located at the horizontal position, the positioning error is the largest, and then with the increase of the absolute value of the vertical angle, the positioning error gradually decreases. When the absolute value of the vertical angle increases to 60 degrees, the positioning error obtained using the proposed linear three-point method is reduced by about 20.9% compared with the positioning error at the horizontal position. This phenomenon occurs mainly because as the absolute value of the vertical angle of the sphere center gradually increases, the horizontal angle measurement range of the sphere contour will also increase, which makes the horizontal angle measurement error of the sphere contour measurement points relatively reduce. Fig. 7 also shows that, compared with the proposed linear three-point method, the proposed maximum likelihood optimization method has a similar positioning effect before the absolute value of the vertical angle of the sphere center is less than 25 degrees. However as the absolute value of the vertical angle continues to increase, the advantage of the parameter optimization method will become more apparent. For example, when the vertical angle of the sphere center position is 60 degrees, the positioning error after the maximum likelihood optimization is reduced by about 7.2% compared with the proposed linear method. It can be observed that the positioning error at different vertical angles of the sphere center can be approximated by a quadratic polynomial equation about the vertical angle.

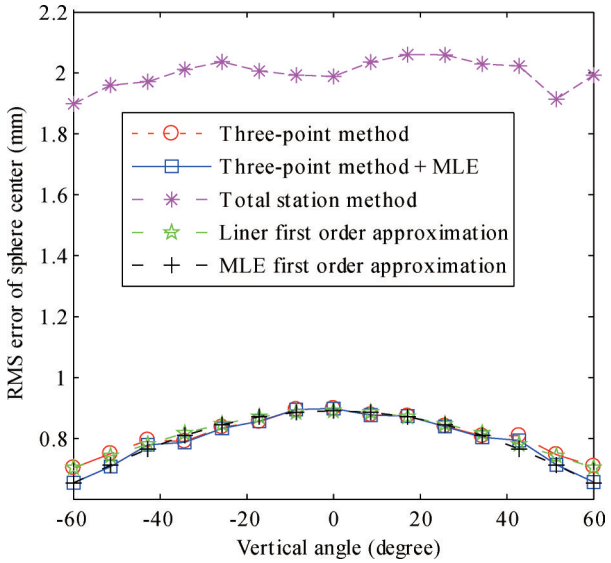

Fig.7 Relationship between vertical angle and sphere center error.

3.5 Empirical Model of Error

From the results of the above simulation experiments, we can see that the first-order approximation of the positioning error of the sphere center is the same as the root mean square error after repeated calculations. Compared with the total station sphere positioning method, the proposed method can significantly improve the positioning accuracy of the sphere center under certain experimental conditions. It is also obvious that the size of the positioning error obtained by the proposed method is more susceptible to the number of contour measurement points, the size of the target sphere, the measurement distance, and the vertical angle of the sphere center. In addition, on the premise that the sphere radius is much smaller than the measuring distance, we can also obtain an empirical model of error based on the above simulation results as

$$Error \approx \frac{D^2}{r\sqrt{N}}\left(9.6876\times10^{-6}-7.2789\times10^{-10}\cdot V_s^2\right) \quad (25)$$

In order to further test the practicability of the sphere center error estimation model, we utilize the model to estimate the sphere center errors under the above four simulation configurations and compare its estimated results with the first-order approximation error previously obtained under the maximum likelihood condition.

It should be noted that when using the total station method for sphere positioning, its positioning error is affected by the angle measurement accuracy and distance measurement accuracy of the instrument. In the short-range measurement environment, the positioning error of the total station is mainly related to the distance measurement accuracy. For a total station with a distance measurement accuracy of 2 mm ± 2 ppm, its positioning error is about 2 mm. It is not difficult to see from the above simulation results that the approximate value is consistent with the error calculated by the simulations.

4 Validation by Real Experiments

In this section we test the sphere center positioning method proposed in this paper by real experiments. In the real experiments, the total station of ZTS-121 is used as the measuring instrument as shown in Fig. 8 (a). Its angle measurement precision is 2″ , and the distance measurement precision is 2 mm ± 2 ppm, where ppm means one-millionth. The test target consists of two standard ceramic balls with diameters of 20.0045 mm and 20.0150 mm, which are fixed on a straight stick with the sphere center distance L = 260.0154 mm, as shown in Fig. 8 (b).

(a) A total station with the angle measurement precision of 2 and the distance measurement precision of 2 mm ± 2 ppm

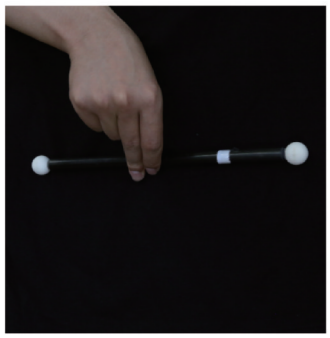

(b) Two standard ceramic balls with the sphere center distance L=260.015 4 mm

Fig.8 The instruments for real experiments

In order to reduce the difference in positioning accuracy caused by different measuring instruments, we use the angle measurement mode of the total station instead of the theodolite with the same angle measurement precision to obtain the latitude-longitude coordinates of the target contour points, and the errors of sphere center distance obtained by the above two methods in different test environments are used as an evaluation standard for positioning accuracy. The operation process of real experiment is as follows:

1) Fix the test target at position 1 with the measuring distance of about 1500 mm and the sphere center vertical angles of about 6 degrees. First, in the angle measurement mode of the total station, 6 contour points are approximately uniformly sampled and measured for the two target balls respectively. Then, use the total station to obtain the three-dimensional coordinates of the marked points of the two target balls respectively. Repeat the test 6 times, and estimate the errors of sphere center distance by using the above two methods.

2) Place the test target at position 2 with a measuring distance of about 1500 mm and the sphere center vertical angles of about −49 degrees. Under different measurement modes, use the total station to perform a measurement similar to step 1) on the two target balls, and estimate the error of sphere center distance.

3) Place the test target at position 3 with a measuring distance of about 2500 mm and the sphere center vertical angles of about 6 degrees. Similarly, use the total station to perform a measurement similar to step 1) on the two target balls, and estimate the error of sphere center distance.

4) Finally, 3 contour points are approximately uniformly sampled and measured for each target ball. Repeat the above operations and estimate the errors of sphere center distance at different positions.

Compared with the traditional total station sphere positioning method, Fig. 9 shows that the sphere center distance obtained using the proposed three-point method is more accurate and reliable under a certain test condition. Moreover, the proposed method is easily affected by the number of contour measurement points, the measuring distance, and the vertical angle of sphere center when positioning a sphere. We can also observe that the proposed three-point method and the maximum likelihood parameter optimization method have similar

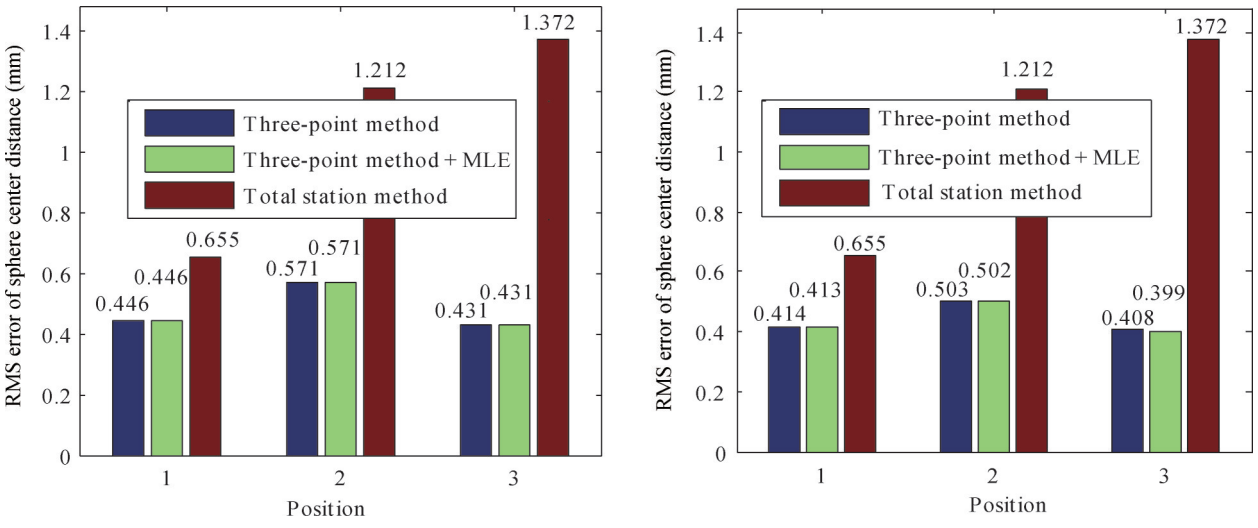

Fig.9 The errors of sphere center distance obtained from real test experiments.
(a)3 contour measurement points are used per target sphere. (b) 6 contour measurement points are used per target sphere.

positioning effects, and when the number of contour measurement points of single sphere is more than 3, the parameter optimization method will more effectively reduce the positioning error with the increase of the absolute value of the vertical angle of the target sphere.

From the above real test experiments, we can conclude that under certain test environments, the proposed sphere positioning method can significantly improve the positioning accuracy of the sphere center compared to the traditional total station method. In practical applications, when the target sphere is fixed at a certain position, we can further reduce the positioning error of the sphere center by increasing the number of contour measurement points and adjusting the height of the measuring instrument. It is consistent with the conclusion obtained by the simulation experiments. In addition, compared with the existing total station sphere positioning method, the proposed method does not need to prepare auxiliary tools in advance, so the cost is lower and the operation is simpler.

5 Conclusion

In this paper, we construct a cylindrical surface model containing the target sphere center based on the known sphere radius and the latitude-longitude coordinates of its contour points in a theodolite, and a novel sphere center positioning algorithm is proposed by using at least three contour points. Since the latitude-longitude coordinates can be measured by a theodolite with low error, the proposed algorithm can effectively reduce the introduction of positioning error.

In simulation experiments, we evaluate and analyze the factors that may affect the positioning accuracy of the sphere center, and obtain the estimation model of the sphere center error. Then, the real experiments are performed. The experimental results show that the proposed three-point method can achieve higher sphere positioning accuracy under certain test conditions, and maximum likelihood optimization is necessary when the absolute value of the vertical angle is relatively large. In the actual measurement, considering the positioning precision and the measurement complexity, we can choose an appropriate number of measurement points for sphere positioning based on the error estimation model.

In summary, the proposed algorithm can utilize high-precision angle measurements from a theodolite to achieve high-precision localization of spheres.

Author Contribution:

Junfeng Sun: Conceptualization, Writing - original draft. Qihua Huang: Data curation, Formal analysis. Lianyou An: Resources, Software, Supervision. Jinling Kang: Validation, Visualization. Baolu Wang: Writing - review & editing. Huanlong Zhang: Data curation, Supervision, Validation.

Declaration of Conflicting Interests

The authors declare that there is no conflict of interest.

Data Availability:

The authors declare that the main data supporting the findings of this study are available within the paper and its Supplementary Information files.

Foundation Information:

This work was supported in part by the National Natural Science Foundation of China under Grants 61703373, 61873246, and U1504604, and in part by the Key research project of Henan Province Universities under Grant 19A413014.

Dates:

Received 18 October 2024; Accepted 20 May 2025; Published online 30 June 2025

References

[1] J. Sun, H. He, and D. Zeng, Global calibration of multiple cameras based on sphere targets, Sensors, vol. 16, no. 1, pp. 77, Jan. **2016**, 10.3390/s16010077. Article (CrossRef Link)

[2] J. Sun, H. He, and D. Zeng, Global calibration of multiple cameras based on sphere targets, Sensors, vol. 16, no. 1, pp. 77, Jan. **2016**, 10.3390/s16010077. Article (CrossRef Link)

[3] Yu, Jian, F. Da, and W. Li. Calibration for Camera–Projector Pairs Using Spheres. IEEE Transactions on Image Processing, vol. 30, pp. 783-793, **2021**. Article (CrossRef Link)

[4] Yang, Fengli, Y. Zhao, and X. Wang. Common Pole-Polar Properties of Central Catadioptric Sphere and Line Images Used for Camera Calibration. International Journal of Computer Vision, vol. 131, pp. 121-133, **2023**. Article (CrossRef Link)

[5] Song, Jin, B. Zeng, and J. Ma. Ellipse detection and positioning in complex vision measurement environments, The Journal of Supercomputing, vol. 81, no. 5, pp. 1-24, **2025**. Article (CrossRef Link)

[6] Y. Li, J. Huo, M. Yang, and G. Zhang, Algorithm of locating the sphere center imaging point based on novel edge model and Zernike moments for vision measurement, Journal of Modern Optics, vol. 66, no. 2, pp. 218-227, Jan. **2019**. Article (CrossRef Link)

[7] J. Gua net al., Extrinsic calibration of camera networks using a sphere, Sensors, vol. 15, no. 8, pp. 18985-19005, Aug. **2015**, Article (CrossRef Link)

[8] R. Penne, B. Ribbens, and P. Roios, An exact robust method to localize a known sphere by means of one image, International Journal of Computer Vision, vol. 127, no. 8, pp. 1012-1024, Aug. **2019**. Article (CrossRef Link)

[9] Y.C. Shiu and S. Ahmad, 3D location of circular and spherical features by monocular model-based vision, in Proc. IEEE ICSMC, Cambridge, MA, USA, **1989**, pp. 576-581. Article

(CrossRef Link)

[10] KYK. Wong, D. Schnieders, and S. Li, Recovering light directions and camera poses from a single sphere, in Proc. *CV-ECCV* , Marseille, France, **2008**, pp. 631-642. Article (CrossRef Link)

[11] K. Shi, X. Li, H. Xu, H. Zhao, and H. Zhang, Sphere localization from a minimal number of points in a single image, in Proc. CTISC, *Xiamen* , China, **2019**, pp. 65-70. Article (CrossRef Link)

[12] M.-C. Kang, C.-H. Yoo, K.-H. Uhm, D.-H. Lee, and S.-J. Ko, A robust extrinsic calibration method for non-contact gaze tracking in the 3-D space, IEEE Access, vol. 6, pp. 48840-48849, Aug. **2018**. Article (CrossRef Link)

[13] J. Huo, Y. Li, and M. Yang, Multi-camera calibration method based on minimizing the difference of reprojection error vectors, Journal Systems Engineering and Electronics, vol. 29, no. 4, pp. 844-853, Aug. **2018**. Article (CrossRef Link)

[14] Z. Tang, Y.-S. Lin, K.-H. Lee, J.-N. Hwang, and J.H. Chuang, ESTHER: Joint camera self-calibration and automatic radial distortion correction from tracking of walking humans, IEEE Access, vol. 7, pp. 10754-10766, Jan. **2019**. Article (CrossRef Link)

[15] Zhang X , Lv T , Dan W , et al. High-precision binocular camera calibration method based on a 3D calibration object, Applied optics, vol. 63, no. 10, pp. 1-16, **2024**. Article (CrossRef Link)

[16] W. Kim, C. Kim and Y. *Cho* et al., A comparative analysis between photogrammetric and auto tracking total station techniques for determining UAV positions, Journal of the Korean Society of Surveying, Geodesy, Photogrammetry and Cartography, vol. 35, no. 6, pp. 553-562, **2017**. Article (CrossRef Link)

[17] E. Osada, M. Owczarek-Wesolowska, and K. Sośnica, Gauss-Helmert model for total station positioning directly in geocentric reference frame including GNSS reference points and vertical direction from earth gravity model, J. Surv. Eng., vol. 145, no. 4, pp. 04019013, **2019**. Article (CrossRef Link)

[18] H. Chen, Y. Wang, and J. Liuet al., Welding ball center positioning method and device, China Patent NO. *CN* 102147242A.

[19] Y. Wen, X. He, Z. Yang, and H. Wang, The location method of single station theodolite under a particular condition, Journal of Projectiles, Rockets, Missiles and Guidance, vol. 29, no. 6, pp. 267-269, Dec. **2009**.

[20] N. Wu, Method for joint positioning of radar and theodolite, Journal of Test and Measurement Technology, vol. 26, no. 5, pp. 452-454, **2012**.

[21] X. Fu, S. Pu, and S. Lei, Moving object location method by individual theodolite in close shot, Journal of Detection & Control, vol. 34, no. 4, pp. 47-51, Aug. **2012**.

[22] Z. Gong, X. Xu, P. Duan, and H. Lei, Research on positioning method of multi-optical theodolites based on Hermite function restriction, Acta Armamentarii, vol. 35, no. 12, pp. 2092-2097, Dec. **2014**.

[23] H. Fang, L. Guo, and X. *Yang* et al., Modular laser 3-dimensional scanning system based on the rotary-laser theodolite positioning network, Opto-Electronic Engineering, vol. 43, no. 6, pp. 57-62, June, 2016. Article (CrossRef Link)

[24] M. Zhao, Photoelectric theodolite intersection positioning method based on fusion dynamic weighting, Electronic Measurement Technology,vol.40, no. 12, pp. 117-120, Dec. **2017**.

[25] H. Stewénius, C. Engels, and D. Nistér, Recent developments on direct relative orientation, ISPRS Journal of Photogrammetry & Remote Sensing, vol. 60, no. 4, pp. 284-294, Jun. **2006**. Article (CrossRef Link)

[26] R. Hartley and A. Zisserman, Levenberg-Marquardt iteration, in Multiple View Geometry in Computer Vision, 2nd ed., New York, USA: Cambridge University Press, **2003**, pp. 600-607.